The characteristics of atmospheric brown carbon in Xi'an, inland China: sources, size distributions and optical properties

Can Wu[1,2], Gehui Wang[1,2,3,4*], Jin Li[2], Jianjun Li[2], Cong Cao[2], Shuangshuang Ge[1], Yuning Xie[1], Jianmin Chen[3,5], Xingru Li[1, 6], Guoyan Xue[1], Xinpei Wang[1], Zhuyu Zhao[7], Fang Cao[7]

[1]Key Lab of Geographic Information Science of the Ministry of Education, School of Geographic Sciences, East China Normal University, Shanghai 210062, China
[2]Key Lab of Aerosol Physics and Chemistry, State Key Laboratory of Loess and Quaternary Geology, Institute of Earth Environment, Chinese Academy of Sciences, Xi'an 710061, China
[3]Institute of Eco-Chongming, 3663 North Zhongshan Road, Shanghai 200062, China
[4]CAS Center for Excellence in Regional Atmospheric Environment, Institute of Urban Environment, Chinese Academy of Sciences, Xiamen 361021, China
[5]Department of Environmental Science and Technology, Fudan University, Shanghai 200433, China
[6]Department of Chemistry, Analytical and Testing Center, Capital Normal University, Beijing 100048, China
[7]Yale-NUIST Center on Atmospheric Environment, Nanjing University of Information Science & Technology, Nanjing 210044, China

[*]Corresponding author. Prof. Gehui Wang
E-mail address: ghwang@geo.ecnu.edu.cn, (Gehui Wang)

Abstract: To investigate the characteristic of atmospheric brown carbon (BrC) in the semi-arid region of East Asia, $PM_{2.5}$ and size-resolved particles in the urban atmosphere of Xi'an, inland China during the winter and summer of 2017 were collected and analyzed for optical properties and chemical compositions. Methanol extracts (MeOH-extracts) were more light-absorbing than water extracts (H_2O- extracts) in the optical wavelength of 300-600 nm, and well correlated with nitrophenols, polycyclic aromatic hydrocarbons (PAHs) and oxygenated PAHs ($r > 0.78$). The light absorptions ($abs_{\lambda=365nm}$) of H_2O- extracts and MeOH-extracts in winter were 28±16 M/m and 49±32 M/m, respectively, which are about 10 times higher than those in summer, mainly due to the enhanced emissions from biomass burning for house heating. Water extracted BrC predominately occurred in the fine mode (< 2.1 μm) during winter and summer, accounting for 81% and 65% of the total absorption of BrC, respectively. The light absorption and stable carbon isotope composition measurements showed an increasing ratio of $abs_{\lambda=365nm}$-MeOH to $abs_{\lambda=550nm}$-EC along with an enrichment of ^{13}C in $PM_{2.5}$ during the haze development, indicating an accumulation of secondarily formed BrC (e.g., nitrophenols) in aerosol aging process. PMF analysis showed that biomass burning, fossil fuel combustion, secondary formation, and fugitive dust are the major sources of BrC in the city, accounting for 55%, 19%, 16%, and 10% of the total BrC of $PM_{2.5}$, respectively.

Key words: Brown Carbon; Haze; Stable carbon isotope composition; Biomass burning; Secondary formation.

1. Introduction

Brown carbon (BrC) is a vital fraction of carbonaceous aerosols, and exhibits strong absorption ability from near ultraviolet (UV) to visible light region. Thus, it has been given extensive investigation in the recent decades (Laskin et al., 2015;Yan et al., 2018;Gustafsson et al., 2009). BrC has significant impact on climate change directly by absorbing solar radiation and indirectly by accelerating snowmelt and affecting the albedo (Qian et al., 2015;Andreae and Ramanathan, 2013). Based on the remote sensing observations and chemical transport models (Chung et al., 2012;Wang et al., 2014;Jo et al., 2016), a non-negligible positive radiative forcing by BrC was found on a global scale with a range from 0.1 to 0.6 W m^{-2}. Beyond that, BrC also influence the atmospheric chemistry and human health. For example, BrC can shield polycyclic aromatic hydrocarbons (PAHs) from being oxidized, and thus substantially elevate lung cancer risk from PAHs (Hsu et al., 2014;Yan et al., 2018).

The sources of BrC are complicated, which can be primarily emitted from incomplete combustion of carbon-containing materials (e.g., biomass, coal and petroleum products.) and secondarily derived from aqueous-phase reaction (Sun et al., 2017;Gilardoni et al., 2016;Xie et al., 2018;Nakayama et al., 2013). Biomass burning was found to be a major source of BrC (Chen and Bond, 2010;Chakrabarty et al., 2010;Saleh et al., 2014), because lignin is of an unsaturated benzene-like structure, which is a chromorphore group. Field measurements and laboratory studies found that BrC is also secondary sources by forming chromophores during the atmosphere ageing process, e.g., high-NOx photooxidation (Liu et al., 2016;Xie et al., 2017), ozonolysis of aromatic precursors (Lee et al., 2014), and aqueous-phase photochemical

oxidation and polymerization (Smith et al., 2014;Flores et al., 2014;Bones et al., 2010). BrC products account for very small weight fraction of organic aerosol (OA), but have a significant effect on OA optical properties. For example, nitroaromatic compounds generated by photooxidation of toluene under high NOx conditions may account for 40-60% of the total light absorption of toluene-SOA (Lin et al., 2015).

Multiple approaches have been developed to quantify the light absorption properties of BrC (Moosmuller et al., 2009), and a common and sensitive approach is the direct measurement of spectrophotometric properties of aerosol water or filter extracts by using optical instrumentation. The advantage of this method can avert interference from insoluble absorption material (e.g., black carbon) (Cheng et al., 2016;Shen et al., 2017), and supply high-resolution spectrum over a wide wavelength coverage. Furthermore, it is favorable for characterization of BrC light-absorbing components by combing with other analytical techniques, such as mass spectrometry (MS) (Laskin et al., 2015;Corr et al., 2012;Satish et al., 2017).

Many studies have been conducted on the BrC optical properties in China, but most of those were based on $PM_{2.5}$ and PM_{10} sample collection and focused on the bulk aerosol optical properties with no information on the size distributions (Shen et al., 2017;Huang et al., 2018). Xi'an is a metropolitan city located in Guanzhong Basin of inland China, which is a typical semiarid region in East Asia and have been suffering from serious particle pollution due to the large emission of anthropogenic pollutants (Wu et al., 2018;Wang et al., 2016;Wu et al., 2019), especially intensive coal combustion and biomass burning in winter for house heating (Wang et al., 2017). In this study, both $PM_{2.5}$ and size-segregated aerosol samples in

Xi'an were collected during the 2017 winter and summer and analyzed for the characteristics of BrC. We firstly investigated the seasonal variations of chemical composition and light-absorption of BrC in the city, then discussed the size distribution of BrC and the impact of aerosol ageing process on BrC, and finally quantified its source contributions.

2. Experimental section

2.1 Sample collection

Aerosol samples were collected on a day/night basis with each for 12-hrs by using a high-volume (~1.13 m^3 min^{-1}) air sampler (Tisch Environmental, Inc., OH, USA) from December 31, 2016 to January 22, 2017 (in winter) and from July 18 to August 6, 2017 (in summer). The sampler was installed on the roof of a three-story building on the campus of the Institute of Earth Environment, CAS (34.22ºN, 108.88ºE), which is located at the urban center of Xi´an, inland China. Meanwhile, size-resolved aerosols with 9 size bins (cutoff points were 0.43, 0.65, 1.1, 2.1, 3.3, 4.7, 5.8, and 9.0 μm, respectively) were collected by using an Anderson sampler at an airflow rate of 28.3 L min^{-1} for 24 hr. All samples were collected onto the pre-baked (450℃ for 6 hr) quartz filters and stored in a freezer (-18℃) prior to analysis.

2.2 Chemical analysis

A punch (0.526 cm^3) from each $PM_{2.5}$ filter sample was analyzed for organic carbon (OC) and elemental carbon (EC) with a DRI Model 2001 Thermal/Optical Carbon Analyzer (Atmoslytic Inc., Calabasas, CA, USA) following the IMPROVE-A protocol (Chow et al., 2007). More details of the method including quality assurance and quality control (QA/QC) can be found elsewhere (Wang et al., 2010).

Partial filters were cut into pieces, and then extracted three times under sonication with

15ml Milli-Q pure water (18.2 MΩ). Ten ions such as SO_4^{2-}, NO_3^-, Cl^-, NH_4^+, and K^+ were determined using ion chromatography (Dionex, ICS-1100). Similar extraction processes were also applied to measure the water-soluble organic carbons (WSOC) of the samples, which was determined by using Shimadz TOC-5000 Carbon Analyzer. The detailed method has been reported by Wang et al. (2013). In order to analyze the organic compounds in the samples such as levoglucosan, PAHs, OPAH and nitrophenols, aliquot of the filter was extracted with a mixture of methanol and DCM (1:5, v/v), derivatized with BSTFA and measured by using gas chromatography (HP 7890A, Agilent Co., USA) coupled with mass spectroscopy detector (GC/MS) (HP 5975, Agilent Co., USA). Details of sample extraction and derivatization were documented elsewhere (Wang et al., 2009b;Ren et al., 2017). Stable carbon isotope composition of total carbon ($\delta^{13}C_{TC}$) was determined by using an elemental analyzer (EA) (Carlo Erba, NA 1500) coupled with an isotope ratio mass spectrometer (IRMS, Finnigan MAT Delta Plus), more details of the method can be referred to elsewhere (Cao et al., 2016).

2.3 Light absorption measurements

Brown carbon (BrC) was extracted from a size of 6 cm^3 filter samples for 30min ultrasonication with 20 ml Milli-Q pure water or methanol. All extracts were then filtered through 0.45 μm PTFE (for water) and 0.22 μm PES (for methanol) pore syringe filter to remove insoluble components and filter debris. The light-absorption spectra were analyzed with a UV–visible spectrophotometer (AOE INSTRUMENTS, China) over a wavelength range of 190–900 nm (Hecobian et al., 2010). The absorption coefficient of water or methanol extracts (M m^{-1}) could be calculated as the following equation (Teich et al., 2017):

$$abs_{\lambda} = (A_{\lambda} - A_{700}) \frac{V_l}{V_a \times L} \times \ln(10) \quad (1)$$

Where A_{λ} and A_{700} were the light absorption of the extracts at the wavelength of λ and 700 nm, respectively. V_l represented the volume of the solvent extracting the filter sample, and V_a was referred to the volume of air corresponding to the filter punch. L was the absorbing path length (i.e., 1 cm for the currently used quartz cuvettes). The ln(10) was converted from base 10 (the form provided by the spectrophotometer) to natural logarithms. According to the previous studies, the absorption coefficient at 365nm was used as the brown carbon absorption in order to avoid disturbance of inorganic salts such as nitrate.

The bulk mass absorption coefficient (MAC, m^2/g) of the extracts at a given wavelength can be described by the following equation:

$$MAC = \frac{abs_{\lambda}}{C_{W(M)SOC}} \quad (2)$$

Where $C_{W(M)SOC}$ was the atmospheric concentration of the particulate water-soluble (WSOC) or methanol-soluble organic carbon (MSOC, $\mu gC/m^3$). In this study, we assumed that OC could be completely dissolved in methanol solvent and substituted the MSOC for the calculation. This hypothesis would possibly lead to somewhat underestimation of the MAC of the methanol extracts, although high extraction efficiency of methanol solvent had been reported by previous studies (Liu et al., 2013) .

The wavelength dependence of light-absorption with respect to the empirically defined power law relationship is described by the following equation (Laskin et al., 2015):

$$MAC = K\lambda^{-AAE} \quad (3)$$

Where K is a factor that includes aerosol mass concentrations, the AAE is termed as absorption Angström exponent. In this study, the AAE value of the filter extracts was determined by a linear regression of log(absλ) versus log(λ) over a wavelength range of 300-450nm.

2.4 Positive Matrix Factorization (PMF) source apportionment

PMF, as a receptor model, decomposes the sample matrix into two matrices (factor contributions and factor profiles), and has been widely used for the source apportionment of atmospheric pollutants. More details on PMF can be found on the EPA website (https://www.epa.gov/air-research/epa-positive-matrix-factorization-50-fundamentals-and-user-guide). In the present work, the mass concentrations of major species (OC, EC, WSOC, SO_4^{2-}, NO_3^-, NH_4^+, Ca^{2+}), organic markers (benzo(b)fluoranthene (BbF), benzo(e)pyrene (BeP),indeno(1,2,3-c,d)pyene (IP), levoglucosan, and nitrophenols), and abs_λ of water extracts have been used as the input data to perform the source apportionment for brown carbon with the EPA PMF 5.0 version, similar reports have been found elsewhere (Hecobian et al., 2010). The model was run numerous times with 3–7 factors and various combinations of the concentration and absorption data set. Base on the Q value (Q_{true} and Q_{robust}) and *r*, which are indicative of the agreement of the model fit, four factors were obtained as the optimal solution.

3. Results and discussion

3.1 Carbonaceous species in $PM_{2.5}$ during summer and winter

Figure 1 shows the temporal variations in the concentrations of $PM_{2.5}$, WSOC, OC and $abs_{\lambda=365nm}$ value during the two seasons. WSOC varied from 5.3 to 67 μgC/m^3 in winter with

188 an average of 23 ± 13 μgC/m^3 (Table 1), which was 4.0 times higher than that in summer. OC
189 exhibited a similar seasonal variation with WSOC with an average of 41 ± 25 μgC/m^3 in
190 winter and 8.4± 2.4 μgC/m^3 in summer, respectively. Whereas, WSOC/OC ratio was much
191 higher in summer (0.70 ± 0.12) than that in winter (0.58 ± 0.13), partly as a result of an
192 enhanced photochemical formation of WSOC under the intense sunlight conditions. Similar
193 phenomena were also found in Beijing (Ping et al., 2017), Shanghai (Zhao et al., 2015a),
194 Tokyo (Miyazaki et al., 2006) and Southeastern United States (Ding et al., 2008).
195 PAHs, OPAHs, and nitrophenols are ubiquitous in the atmosphere, which can be directed
196 emitted from incomplete combustion of carbon -containing fuels (e.g., coal, biomass) (Shen et
197 al., 2013;Zhang and Tao, 2009). In addition, OPAHs and nitrophenols can also be produced
198 from photochemical reactions (Cochran et al., 2016;Keyte et al., 2013;Yuan et al., 2016).
199 These compounds are the efficient light-absorbing species, because their molecular structures
200 consist of chromophores (Lin et al., 2017;Bluvshtein et al., 2017). Herein, 14 PAHs, 7 OPAHs,
201 and 7 nitrophenols were examined for investigating their effect on BrC absorption. As seen in
202 Figure S1, the temporal variations of PAHs, OPAHs, and nitrophenols were similar with
203 levoglucosan, which is the tracer of biomass burning emissions, indicating that biomass
204 burning is one of the major sources of these compounds. Concentrations of PAHs, OPAHs,
205 and nitrophenols during winter were 149 ± 89 ng/m^3, 174 ± 98 ng/m^3 and 17 ± 12 ng/m^3
206 (Table 1), respectively, and were 10 - 43 times higher than those in summer, which can be
207 explained by an increasing emission from residential heating during winter in the city and its
208 surrounding regions.
209 As shown in Table S1, $abs_{\lambda=365nm}$ extracted by methanol displays showed well correlations

with PAHs, OPAHs, and nitrophenols, especially in winter ($r > 0.89$), which suggests that those species are important light absorption contributors for BrC in Xi'an. Huang et al. (2018) found that PAHs and OPAHs in Xi'an accounted for, on average, 1.7% of the overall absorption of methanol-soluble BrC, but their mass fraction in OC was only 0.35%. A recent study reported that biomass burning also emitted nitroaromatic compounds, particularly nitrophenols, and accounted for 50-80% of the total visible light absorption (> 400 nm) (Lin et al., 2017). The robust correlations of above compounds with the absorption at λ=365 nm suggest that PAHs, OPAHs and nitrophenol are strong light-absorbing species.

3.2 Light absorption of BrC in water and methanol extracts

3.2.1 Seasonal variations of light absorption by BrC

As shown in Figure 2a and 2b, the marked feature of BrC in Xi'an is that the absorption spectrum increased notably from the visible to the ultraviolet ranges, and the average abs-MeOH at λ=365 nm was 1.5 - 1.7 times higher than abs-H_2O in the two seasons, indicating that MSOC provided a more comprehensive estimation for BrC. Due to enhanced emission of BrC, average $abs_{\lambda=365nm}$ of BrC found in winter was 49 ± 32 M/m for MeOH and 28 ± 16 M/m for WSOC, which were 9.5- and 8.1-fold higher than that in summer. This phenomenon was also observed in previous studies in Xi'an (Shen et al., 2017;Huang et al., 2018) and other areas of China (Du et al., 2014;Chen et al., 2018). Compared with other regions (Table 2), the absolute $abs_{\lambda=365nm}$ values in Xi'an were slightly lower than that in Indo-Gangetic Plain, India (Satish et al., 2017;Bachi, 2016), but were considerably higher than those in Beijing, China (Du et al., 2014), US (Zhang et al., 2011) and Korea (Kim et al., 2016), suggesting a heavy pollution of light-absorbing aerosols in Xi'an. Furthermore,

232 enhanced $abs_{\lambda=365nm}$ loading in the nighttime was observed during the two seasons, which can
233 be ascribed to the shallower boundary layer height and the absence of photo-bleaching
234 processes at night (Saleh et al., 2013;Zhao et al., 2015b).
235 Linear regression slopes on the scatter plots of $abs_{\lambda=365nm}$ values versus WSOC or MSOC
236 represented the average of MAC at 365 nm (i.e., MAC_{WSOC} and MAC_{MSOC}). During winter,
237 there was a slight disparity between the MAC_{WSOC} and MAC_{MSOC} with the averages of 1.2 ±
238 0.06 and 1.3 ± 0.03 m^2/g (Figure 2e), respectively, which indicates that there are some similar
239 chromophores of BrC between the two fractions. As seen in Table 2, both MAC_{WSOC} and
240 MAC_{MSOC} in Xi'an during the two seasons are higher than those in US and Korea, suggesting
241 that BrC in the city was comprised of stronger light-absorbing compounds. $abs_{\lambda=365nm}$ showed
242 a strong linear correlation with levoglucosan ($r > 0.98$), suggesting that abundant BrC was
243 largely derived from biomass burning. As shown in Fig. S2, mass ratios of
244 levoglucosan/mannosan and levoglucosan/galacosan in the $PM_{2.5}$ samples are similar to
245 biomass types (i.e., woods, leaves, wheat straw), again reflecting that biomass burning
246 combustion in Xi'an and its surrounding regions are probably the major sources of BrC in the
247 city during winter. Compared to winter, the MAC in summer was slightly lower, which can be
248 in part attributed to the less abundant light-absorbing PAHs and OPAHs due to no biomass
249 burning for house heating. Moreover, with increasing photooxidation in summer,
250 fragmentation reactions would occur and thus decrease light absorption for BrC aerosols, as
251 reported by Sumlin et al. (2017), because higher levels of O_3 and OH radicals in summer
252 intensify the photooxidation and diminish the BrC aerosol light absorption by reducing the
253 size of conjugated molecular systems. Interestingly, we found that the MAC_{WSOC} (1.1 ± 0.2

m^2/g) in summer was significantly enhanced compared to MAC_{MSOC} (0.8 ± 0.1 m^2/g), which can be ascribed to more amount of non-BrC in the methanol extracts such as phthalates, of which the abundance relative to OC was about 10 time higher in summer than in winter. The $abs_{\lambda=365nm}$ showed a poor correlation with levoglucosan (Table S1), further indicating that the biomass burning was not the dominant source for BrC in summer.

Absorption Ångström exponents (AAE), which were derived from the filter methanol- and water-extracted BrC (AAE_{WSOC} and AAE_{MSOC}) for wavelengths between 300 and 450 nm, were 6.1 ± 9.7 and 5.3 ± 8.5 (Table 2) in winter, respectively, and resembled that in Beijing (Cheng et al., 2016), Guangzhou (Liu et al., 2018) and Indo- Gangetic Plain (Bachi, 2016), possibly indicating that the chemical compositions of BrC chromophores in these regions are similar during winter. As seen in Table 2, unlike those of H_2O-extracts, the averaged values of MAC and AAE of MeOH extracts were 40% and 10% higher in winter than in summer, respectively, suggesting that chemical compositions of BrC are different between the two seasons in the city and the winter BrC contained more non-polar compounds that are of stronger light-absorbing ability.

3.2.2 Aerosol size distribution of BrC

Particles with different sizes are of different chemical compositions, and thus optical properties of BrC in different size of particles are also different (Zhang et al., 2015;Zhai et al., 2017). However, information on size distribution of BrC absorption is very limited. In this study, we mainly focused on the water-extracted samples, because particles deposited on the filter surface are unevenly distributed, making the quantifications of OC and EC in the size-segregated samples not accurate enough. As shown in Figure S3, there was a good

relationship between the $abs_{\lambda=365nm}$ ($r > 0.98$) of the samples collected by Anderson sampler and those collected by high-volume $PM_{2.5}$ sampler (Fig. S3), suggesting a good agreement between the two sampling methods.

As show in Figure 3, $abs_{\lambda=365nm}$ presented a bimodal pattern during winter and summer, dominating at the fine mode (Dp <2.1μm) with relative contributions of 81% and 65% to the total absorption in the two seasons, respectively. These proportions are similar to those reported for a forest wildfire event, which showed that 93% of the total BrC absorption was in the fine particles (0.10 < Dp < 1.0 μm) (Lorenzo et al., 2018). Maximum absorptions were observed at 1.02 and 0.71μm (Dpg- geometric mean diameters, Figure 3a and 3b) in winter and summer, respectively, which is in agreement with the observations by Lei et al (2018), who found that the major peaks for BrC absorption were in the rang from 0.5μm to 1.0μm in urban and may shift toward smaller size (< 0.4μm) for particles released from burning experiments (Lei et al., 2018). However, the size distribution pattern of MAC was different from that of $abs_{\lambda=365nm}$ in Xi'an, which presented a monomodal distribution with a peak in the fine mode (<2.1μm) in winter and a bimodal distribution in summer with two peaks in the fine (<2.1μm) and coarse (>2.1μm) modes, respectively (Figure 3c and 3d). As seen in Figure 3c and 3d, the fine mode of MAC was around 50% larger in winter than that in summer, suggesting that water-soluble fraction of winter fine particles was more light-absorbing compared to that in summer, probably due to the summertime stronger bleaching effect.

3.3 Underestimation of BrC absorption by solvent extraction methods

A few studies pointed out that absorption properties of BrC extracted by bulk solution may not entirely reflect the light absorption by ambient aerosols. Here, we further calculated

298 the light absorption of the samples using the Mie theory combined with an imaginary (*k*,
299 responsible for absorption) refractive index with assumptions that particles were of spherical
300 morphology and externally mixed with other light-absorbing components. The imaginary
301 refractive index could be obtained from MAC using follow equation (Laskin et al., 2015):

$$k_{(\lambda)}=\frac{\rho\,\lambda\,abs}{4\pi\times WSOC}=\frac{\rho\,\lambda\,MAC}{4\pi} \quad (4)$$

302 Where ρ (g/cm^3) was particle density and assigned as 1.5, more details about Mie
303 calculations can be referred to the study by Liu et al. (2013).

304 As noted above, most BrC aerosols were in the fine mode (<2.1μm), thus, here we only
305 focused on this fraction for the Mie calculations. The values of imaginary refractive in winter
306 remains nearly constant (0.038-0.048) for different particle sizes at λ=365 nm (Table 3),
307 which was about two times smaller than that (0.093 ± 0.049) over Gangetic Plain, India
308 (Shamjad et al., 2017). Values of *k* in summer were slight smaller when compared to those in
309 winter, suggesting that the aerosols in summer were more aged. Sumlin et al. (2017) found
310 that *k* decreases along with the atmospheric aging from 0.029 ± 0.001 to 0.019 ± 0.001 at
311 λ=375 nm. However, *k* values in this study were 5.0 times (avg.) higher than those reported
312 from the United States (Liu et al., 2013). This is because that $PM_{2.5}$ particles in Xi'an, China
313 are enriched in BrC and the mass absorption coefficient was considerably higher than that in
314 US. Figure 4 compares the difference between $abs_{\lambda=365nm}$ predicted by Mie theory (abs-Mie)
315 and that extracted by the bulk solution (abs-Measure). Mie theory predicted $abs_{\lambda=365nm}$ was
316 1.5-fold higher than that measured by the bulk solution, suggesting that the solvent extraction
317 methods, which have commonly been used for atmospheric BrC measurements, could result

in an underestimation on optical absorption of aerosols. Hence, a factor of 1.5 is recommended to convert the liquid-based data (at least for the water-soluble data) reported by this work for estimating optical properties of atmospheric aerosols in Xi'an and its surrounding regions in order to better quantify the BrC light-absorption.

3.4 The characteristic of BrC with the aerosol aging

During the ageing process, secondary organic aerosols (SOA) with strong chromophores can be generated and efficiently absorb solar radiation (Lin et al., 2014;Lin et al., 2016). From Figure 5, it can be found that air quality in Xi'an during the winter varied from the clean ($PM_{2.5}$ < 75 μg/m^3) to the polluted conditions ($PM_{2.5}$ > 75 μg/m^3) from the period of 12th January to 19th January. Such a case provides an opportunity to investigate the changes in light-absorption by BrC during the aerosol ageing process.

As shown in Figure 5a and 5b, $abs_{\lambda=365nm}$ extracted by water and MeOH in Xi'an during the campaign showed an increasing trend from 12th January to 19th January, which is similar to $PM_{2.5}$ loadings but opposite to the visibility, indicating that BrC is one of the important factors leading to the visibility deterioration. From Figure 5b, it can also be seen that light absorption of water-extracts dominated over the total BrC absorption especially in daytime and showed a variation pattern similar to the $PM_{2.5}$ (Figure 5a) and WSOC loadings (Figure 5c), indicating a continuous formation of secondary BrC during the aerosol ageing process. To illustrate this point, the stable carbon isotopic composition ($\delta^{13}C_{TC}$) of total carbon (TC) in the samples was measured. WSOC/OC showed a positive correlation with the $\delta^{13}C_{TC}$, demonstrating an ageing process of aerosols during the haze development from 12th to 19th, January, although it was weak (r = 0.47, n = 17). Similar conclusions were also reported by

Yang et al. (2004) and Pavuluri et al. (2015). From Figure 5c, increasing trends of OPAHs and nitrophenols were observed during the haze development, suggesting that more SOAs with chromophores were generated during such an aerosol ageing process, because these compounds are also of secondary origins. To exclude the possible impact of the changes in BrC source emissions, the values of PAHs/OC and levoglucosan/OC were applied in this study, because PAHs and levoglucosan emission factors are different for different sources(Nguyen-Duy and Chang, 2017). As shown in Fig. S4, both values indistinctively changed during the aerosol ageing process, indicating that the increasing $abs_{\lambda=365nm}$ were not caused by the changes in source emissions. Moreover, we found that MAC_{MSOC} values during the age process also increased (Figure 5a), further suggesting that the bleaching effect on light-absorbing BrC was reducing during the haze developing process.

EC is one of the major light-absorbing aerosols in the atmosphere (Collier et al., 2018;Peng et al., 2016). To further discuss the changes of BrC during the aerosol ageing process, we compared the mass absorption efficiency of EC at λ=550 nm (7.5 ± 1.2 m^2/g) with BrC by using the method reported from Yan et al. (2015) and Kirillova et al. (2014). As shown in Figure 5c, the concentrations of EC have a slight change in the haze period, so the changes in light absorption of EC remained nearly constant. However, the ratio of $abs_{\lambda=365nm}$-MeOH/$abs_{\lambda=550nm}$-EC increasingly became larger along with the visibility deterioration from January 12th to January 19th (Fig. 5b), while the mass ratios of PAHs/EC, OPAHs/EC and nitrophenols /EC during the period showed a significant negative correlation with visibility (Fig. S5), further suggesting that the impairment of BrC on the visibility was getting more significant during the haze development process.

During the haze developing process, organic aerosols are usually getting more aged and enriched in heavier ^{13}C due to the kinetic isotopic effect (KIE) (Wang et al., 2010). As shown in Figure 6a and b, $\delta^{13}C$ of $PM_{2.5}$ samples presented a strong positive correlation with $abs_{\lambda=365\ nm}$-MeOH (r=0.82) in the daytime, while there was no such a correlation in the nighttime during the haze period of January 12th -19th, indicating a daytime formation of secondary BrC. From Figure 6c and 6d, we also found that the correlation of $abs_{\lambda=365\ nm}$-MeOH/ $abs_{\lambda=550\ nm}$-EC ratio with nitrophenol was much stronger in daytime than in nighttime, which is opposite to the correlation of $abs_{\lambda=365\ nm}$-MeOH/ $abs_{\lambda=550\ nm}$-EC ratio with PAHs. Nitrophenols can be produced from secondary photooxidation of phenol with NOx, while PAHs are produced solely from direct emissions especially from coal and biomass burning for house heating. The opposite diurnal correlations of $abs_{\lambda=365\ nm}$-MeOH/ $abs_{\lambda=550\ nm}$-EC ratio with nitrophenols and PAHs again revealed an enhanced formation of secondary BrC during the aerosol ageing process.

3.5 Positive matrix factorization (PMF) analysis for BrC source apportionment

In the current work, The EPA PMF 5.0 model was used for identifying the possible sources of BrC. Because the number of the collected samples in each season was not large enough, data from the two seasons were merged together to form a dataset of 80 × 12 (80 samples with 12 species) in order to obtain an accurate analysis according to the PMF user guide. The resolved source profiles (factors) represented the sources that influenced variability in the selected components throughout two seasons in Xi'an. Similar approach was also reported by Zhang et al. (2010). With several iterative testes, a solution with four factors was identified as the optimal solution. As shown in Table S2, the values of Q_{true} and Q_{robust}

were consistent, which indicates that the model fits the input data well. Furthermore, the correlation coefficient between input and model values ranged from 0.82 to 0.99 with an average 0.96, also implying that the model fit well. This assess method was widely used in previous studies (Ren et al., 2017;Wang et al., 2009a).

Figure7 shows the factor profiles resolved by the model. Factor 01 was characterized by high levels of BeF (52%), BeP (57%), and IP (67%), which were primarily derived from coal combustion and vehicle exhausts (Kong et al., 2010;Ma et al., 2010;Harrison et al., 1996), further, relatively high OC (29%) and EC (25%) associated with this factor was well known tracers of exhaust emissions (Zong et al., 2016), so we identified Factor 01as the source from fossil fuel combustion. Factor 02 (fugitive dust) shows high contribution of Ca^{2+} (69%) and a moderate loading of EC (39%). Ca, as one of the most abundant crustal elements, is largely from construction work, resuspended dust or soil sources (Chow et al., 2004;Han et al., 2007). In addition, EC was a well-known tracer of vehicular emissions (Dorado et al., 2003), so this factor can be attributed to the impact of vehicles passing with higher speeds, leading to resuspend non-tailpipe particles. Moreover, the concentrations of Ca^{2+} in the night were almost higher than that during the day time, with averages of 1.8 ± 1.56 and 1.43 ±0.85 μg/m^3, respectively. This is consistent with time for transporting the construction wastes by lorry. Thus, factor 02 was identified as fugitive dust. Factor 03 was identified as secondary formation, as it is associated with high loadings of NO_3^- (63%), SO_4^{2-} (73%), NH_4^+ (69%) and a moderate loading of OC and WSOC, indicating the presence of secondary inorganic and organic aerosols. The factor 04 showed high loadings with nitrophenols, levoglucosan, and abs-MeOH and was identified as biomass burning, because levoglucosan is the tracer for

biomass burning smoke, and nitrophenols can be produced in the aging process of biomass burning plume.

Figure 8 shows the contributions of the above sources to the light absorption at λ=365nm, which also represents the fraction of BrC for the factors. Biomass burning was the primary source of the BrC, accounting for 55% of the total BrC in the city, which is coincided with the results discussed in the section 3.2.1. A significant fraction (about 19%) of BrC was associated with fossil fuel combustion. The fraction of secondary BrC was about 16%, which was enhanced during the summer due to the efficient photochemical formation of secondary chromophores. The AAE value of total BrC, closed to the aged SOA-AAE (4.7-5.3) (Bones et al., 2010), can also verify it. The remaining fraction of BrC was derived from the fugitive dust in the city. The results of BrC source apportionment for the Xi'an samples are in line with the work by Shen et al. (2017) and also similar to the results obtained in Beijing by using radiocarbon fingerprinting (Yan et al., 2017).

4. Conclusions

This study investigated the seasonality of the light-absorption characteristics of BrC in Xi'an. Light absorption coefficient (MAC) of methanol-extracts at 365nm was 1.5-1.7 folds higher than that of water-extracts in the two seasons, suggesting non-polar compounds in the city are of stronger light-absorbing ability than that of polar compounds. The strong correlation of levoglucosan with BrC and the diagnostic ratios of levoglucosan/mannosan and levoglucosan/galacosan revealed that the wintertime abundant BrC ($abs_{\lambda=365nm}$-MeOH of 49.18 ± 31.67 M/m) in Xi'an was mainly derived from the residential biofuel combustion for house heating in the city and its surrounding region. Size distribution results showed that 81%

and 65% of BrC occurred in the fine mode (< 2.1μm) during winter and summer, respectively, which is characterized by a monomodal size distribution with a peak in winter and a bimodal size distribution in summer with two peaks in the fine and coarse modes, respectively. The fine mode of MAC is 50% higher in winter than that in summer, suggesting that the light-absorbing ability of wintertime fine particles is stronger, due to the abundant occurrence of PAHs and other aromatic compounds in the fine mode.

The linear correlation between the ratio of $abs_{\lambda=365nm}$-MeOHO/$abs_{\lambda=550nm}$-EC and the enrichment of ^{13}C during the haze development indicated an accumulation of secondary BrC in the aerosol ageing process. The daytime strong correlation of the ratio of $abs_{\lambda=365nm}$-MeOHO/$abs_{\lambda=550nm}$-EC with nitrophenols in the haze event further revealed that such an enhanced production of secondary BrC is related to the photooxidation of aromatic compounds with NOx. Source apportionment by using PMF showed that 55% of the BrC was associated with biomass burning in the city during the campaign, with 19 and 16% of BrC derived from fossil fuel combustion and secondary formation, respectively.

Author contributions. GW designed the experiment. CW, JianjunL, JinL and CC collected the samples. CW and ZZ conducted the experiments. CW and GW performed the data interpretation and wrote the paper. All authors contributed to the paper with useful scientific discussions or comments.

Competing interests. The authors declare that they have no conflict of interest.

Acknowledgements. This work was financially supported by National Key R&D Plan (Quantitative Relationship and Regulation Principle between Regional Oxidation Capacity of Atmospheric and Air Quality (No. 2017YFC0210000), the program from National Nature Science Foundation of China (No. 41773117).

References

Andreae, M. O., and Ramanathan, V.: Climate change. Climate's dark forcings, Science, 340, 280-281, 10.1126/science.1235731, 2013.

Bachi, S.: Mass absorption efficiency of light absorbing organic aerosols from source region of paddy-residue burning emissions in the Indo-Gangetic Plain, Atmospheric Environment, 125, 360-370, 10.1016/j.atmosenv.2015.07.017, 2016.

Bluvshtein, N., Lin, P., Flores, J. M., Segev, L., Mazar, Y., Tas, E., Snider, G., Weagle, C., Brown, S. S., and Laskin, A.: Broadband optical properties of biomass burning aerosol and identification of brown carbon chromophores, Journal of Geophysical Research, 122, 10.1002/2016JD026230, 2017.

Bones, D. L., Henricksen, D. K., Mang, S. A., Gonsior, M., Bateman, A. P., Nguyen, T. B., Cooper, W. J., and Nizkorodov, S. A.: Appearance of strong absorbers and fluorophores in limonene-O3secondary organic aerosol due to NH4+-mediated chemical aging over long time scales, Journal of Geophysical Research, 115, 10.1029/2009jd012864, 2010.

Cao, F., Zhang, S.-C., Kawamura, K., and Zhang, Y.-L.: Inorganic markers, carbonaceous components and stable carbon isotope from biomass burning aerosols in Northeast China, Science of the Total Environment, 572, 1244-1251, 10.1016/j.scitotenv.2015.09.099, 2016.

Chakrabarty, R. K., Moosmüller, H., Chen, L. W. A., and Lewis, K.: Brown carbon in tar balls from smoldering biomass combustion, Atmospheric Chemistry and Physics, 10, 6363-6370, 10.5194/acp-10-6363-2010, 2010.

Chen, Y., and Bond, T. C.: Light absorption by organic carbon from wood combustion, Atmospheric Chemistry & Physics Discussions, 9, 1773-1787, 10.5194/acp-10-1773-2010, 2010.

Chen, Y., Ge, X., Chen, H., Xie, X., Chen, Y., Wang, J., Ye, Z., Bao, M., Zhang, Y., and Chen, M.: Seasonal light absorption properties of water-soluble brown carbon in atmospheric fine particles in Nanjing, China, Atmospheric Environment, 230-240, 10.1016/j.atmosenv.2018.06.002, 2018.

Cheng, Y., He, K. B., Du, Z. Y., Engling, G., Liu, J. M., Ma, Y. L., Zheng, M., and Weber, R. J.: The characteristics of brown carbon aerosol during winter in Beijing, Atmospheric Environment, 127, 355-364, 10.1016/j.atmosenv.2015.12.035, 2016.

Chow, J. C., Watson, J. G., Kuhns, H., Etyemezian, V., Lowenthal, D. H., Crow, D., Kohl, S. D., Engelbrecht, J. P., and Green, M. C.: Source profiles for industrial, mobile, and area sources in the Big Bend Regional Aerosol Visibility and Observational study, Chemosphere, 54, 185-208, 10.1016/j.chemosphere.2003.07.004, 2004.

Chow, J. C., Watson, J. G., Chen, L. W., Chang, M. C., Robinson, N. F., Trimble, D., and Kohl, S.: The IMPROVE_A temperature protocol for thermal/optical carbon analysis: maintaining consistency with a long-term database, Journal of the Air & Waste Management Association, 57, 1014-1023, 10.3155/1047-3289.57.9.1014, 2007.

Chung, C. E., Ramanathan, V., and Decremer, D.: Observationally-constrained Estimates of Carbonaceous Aerosol Radiative Forcing, PROCEEDINGS OF THE NATIONAL ACADEMY OF SCIENCES OF THE

498 UNITED STATES OF AMERICA, 109, 11624-11629, 10.1073/pnas.1203707109, 2012.
499 Cochran, R. E., Jeong, H., Haddadi, S., Fisseha Derseh, R., Gowan, A., Beránek, J., and Kubátová, A.:
500 Identification of products formed during the heterogeneous nitration and ozonation of polycyclic aromatic
501 hydrocarbons, Atmospheric Environment, 128, 92-103, 10.1016/j.atmosenv.2015.12.036, 2016.
502 Collier, S., Williams, L. R., Onasch, T. B., Cappa, C. D., Zhang, X., Russell, L. M., Chen, C.-L., Sanchez, K. J.,
503 Worsnop, D. R., and Zhang, Q.: Influence of Emissions and Aqueous Processing on Particles Containing
504 Black Carbon in a Polluted Urban Environment: Insights From a Soot Particle-Aerosol Mass Spectrometer,
505 Journal of Geophysical Research-Atmospheres, 123, 6648-6666, 10.1002/2017jd027851, 2018.
506 Corr, C. A., Hall, S. R., Ullmann, K., and Anderson, B. E.: Spectral absorption of biomass burning aerosol
507 determined from retrieved single scattering albedo during ARCTAS, Atmospheric Chemistry and Physics,
508 12, 10505-10518, 10.5194/acp-12-10505-2012, 2012.
509 Ding, X., Zheng, M., Yu, L., Zhang, X., Weber, R. J., Yan, B., Russell, A. G., Edgerton, E. S., and Wang, X.:
510 Spatial and Seasonal Trends in Biogenic Secondary Organic Aerosol Tracers and Water-Soluble Organic
511 Carbon in the Southeastern United States, Environmental Science & Technology, 42, 5171-5176,
512 10.1021/es7032636, 2008.
513 Dorado, M. P., Ballesteros, E., Arnal, J. M., Gómez, J., and López, F. J.: Exhaust emissions from a Diesel engine
514 fueled with transesterified waste olive oil ☆, Fuel, 82, 1311-1315, 10.1016/S0016-2361(03)00034-6, 2003.
515 Du, Z., He, K., Cheng, Y., Duan, F., Ma, Y., Liu, J., Zhang, X., Zheng, M., and Weber, R.: A yearlong study of
516 water-soluble organic carbon in Beijing II: Light absorption properties, Atmospheric Environment, 89,
517 235-241, 10.1016/j.atmosenv.2014.02.022, 2014.
518 Flores, J. M., Washenfelder, R. A., Adler, G., Lee, H. J., Segev, L., Laskin, J., Laskin, A., Nizkorodov, S. A.,
519 Brown, S. S., and Rudich, Y.: Complex refractive indices in the near-ultraviolet spectral region of biogenic
520 secondary organic aerosol aged with ammonia, Physical Chemistry Chemical Physics, 16, 10629-10642,
521 10.1039/c4cp01009d, 2014.
522 Gilardoni, S., Massoli, P., Paglione, M., Giulianelli, L., Carbone, C., Rinaldi, M., Decesari, S., Sandrini, S.,
523 Costabile, F., Gobbi, G. P., Pietrogrande, M. C., Visentin, M., Scotto, F., Fuzzi, S., and Facchini, M. C.:
524 Direct observation of aqueous secondary organic aerosol from biomass-burning emissions, Proceedings of
525 the National Academy of Sciences of the United States of America, 113, 10013-10018,
526 10.1073/pnas.1602212113, 2016.
527 Gustafsson, O., Kruså, M., Zencak, Z., Sheesley, R. J., Granat, L., Engström, E., Praveen, P. S., Rao, P. S., Leck,
528 C., and Rodhe, H.: Brown clouds over South Asia: biomass or fossil fuel combustion?, Science, 323,
529 495-498, 10.1126/science.1164857, 2009.
530 Han, L., Zhuang, G., Cheng, S., Wang, Y., and Li, J.: Characteristics of re-suspended road dust and its impact on
531 the atmospheric environment in Beijing, Atmospheric Environment, 41, 7485-7499,
532 10.1016/j.atmosenv.2007.05.044, 2007.
533 Harrison, R. M., Smith, D. J. T., and Luhana, L.: Source Apportionment of Atmospheric Polycyclic Aromatic
534 Hydrocarbons Collected from an Urban Location in Birmingham, U.K, Environmental Science &
535 Technology, 30, 825-832, 10.1021/es950252d, 1996.
536 Hecobian, A., Zhang, X., Zheng, M., Frank, N., Edgerton, E. S., and Weber, R. J.: Water-Soluble Organic
537 Aerosol material and the light-absorption characteristics of aqueous extracts measured over the
538 Southeastern United States, Atmospheric Chemistry and Physics, 10, 5965-5977,
539 10.5194/acp-10-5965-2010, 2010.
540 Hsu, H. I., Lin, M. Y., Chen, Y. C., Chen, W. Y., Yoon, C., Chen, M. R., and Tsai, P. J.: An integrated approach to

assess exposure and health-risk from polycyclic aromatic hydrocarbons (PAHs) in a fastener manufacturing industry, International Journal of Environmental Research & Public Health, 11, 9578-9594, 10.3390/ijerph110909578, 2014.

Huang, R. J., Yang, L., Cao, J., Chen, Y., Chen, Q., Li, Y., Duan, J., Zhu, C., Dai, W., and Wang, K.: Brown Carbon Aerosol in Urban Xi'an, Northwest China: The Composition and Light Absorption Properties, Environmental Science & Technology, 52, 6825-6833 10.1021/acs.est.8b02386, 2018.

Jo, D. S., Park, R. J., Lee, S., Kim, S. W., and Zhang, X. L.: A global simulation of brown carbon: implications for photochemistry and direct radiative effect, Atmospheric Chemistry and Physics, 16, 3413-3432, 10.5194/acp-16-3413-2016, 2016.

Keyte, I. J., Harrison, R. M., and Lammel, G.: Chemical reactivity and long-range transport potential of polycyclic aromatic hydrocarbons - a review, Chemical Society Reviews, 42, 9333-9391, 10.1039/c3cs60147a, 2013.

Kim, H., Jin, Y. K., Jin, H. C., Ji, Y. L., and Lee, S. P.: Seasonal variations in the light-absorbing properties of water-soluble and insoluble organic aerosols in Seoul, Korea, Atmospheric Environment, 129, 234-242, 10.1016/j.atmosenv.2016.01.042, 2016.

Kirillova, E. N., Andersson, A., Tiwari, S., Srivastava, A. K., Bisht, D. S., and Örjan, G.: Water-soluble organic carbon aerosols during a full New Delhi winter: Isotope-based source apportionment and optical properties, Journal of Geophysical Research Atmospheres, 119, 3476-3485, 10.1002/2013JD020041, 2014.

Kong, S., Ding, X., Bai, Z., Han, B., Chen, L., Shi, J., and Li, Z.: A seasonal study of polycyclic aromatic hydrocarbons in PM(2.5) and PM(2.5-10) in five typical cities of Liaoning Province, China, J Hazard Mater, 183, 70-80, 10.1016/j.jhazmat.2010.06.107, 2010.

Laskin, A., Laskin, J., and Nizkorodov, S. A.: Chemistry of atmospheric brown carbon, Chem Rev, 115, 4335-4382, 10.1021/cr5006167, 2015.

Lee, H. J., Aiona, P. K., Laskin, A., Laskin, J., and Nizkorodov, S. A.: Effect of solar radiation on the optical properties and molecular composition of laboratory proxies of atmospheric brown carbon, Environmental Science & Technology, 48, 10217-10226, 10.1021/es502515r, 2014.

Lei, Y., Shen, Z., Zhang, T., Zhang, Q., Wang, Q., Sun, J., Gong, X., Cao, J., Xu, H., and Liu, S.: Optical source profiles of brown carbon in size-resolved particulate matter from typical domestic biofuel burning over Guanzhong Plain, China, Science of the Total Environment, 622, 244-251, 10.1016/j.scitotenv.2017.11.353, 2018.

Lin, G., Penner, J. E., Flanner, M. G., Sillman, S., Xu, L., and Zhou, C.: Radiative forcing of organic aerosol in the atmosphere and on snow: Effects of SOA and brown carbon, Journal of Geophysical Research: Atmospheres, 119, 7453-7476, 10.1002/2013jd021186, 2014.

Lin, P., Liu, J., Shilling, J. E., Kathmann, S. M., Laskin, J., and Laskin, A.: Molecular characterization of brown carbon (BrC) chromophores in secondary organic aerosol generated from photo-oxidation of toluene, Phys Chem Chem Phys, 17, 23312-23325, 10.1039/c5cp02563j, 2015.

Lin, P., Aiona, P. K., Li, Y., Shiraiwa, M., Laskin, J., Nizkorodov, S. A., and Laskin, A.: Molecular Characterization of Brown Carbon in Biomass Burning Aerosol Particles, Environmental Science & Technology, 50, 11815-11824, 10.1021/acs.est.6b03024, 2016.

Lin, P., Bluvshtein, N., Rudich, Y., Nizkorodov, S. A., Laskin, J., and Laskin, A.: Molecular Chemistry of Atmospheric Brown Carbon Inferred from a Nationwide Biomass Burning Event, Environmental Science & Technology, 51, 11561-11570, 10.1021/acs.est.7b02276, 2017.

Liu, J., Bergin, M., Guo, H., King, L., Kotra, N., Edgerton, E., and Weber, R. J.: Size-resolved measurements of

584 brown carbon in water and methanol extracts and estimates of their contribution to ambient fine-particle
585 light absorption, Atmospheric Chemistry and Physics, 13, 12389-12404, 10.5194/acp-13-12389-2013, 2013.
586 Liu, J., Lin, P., Laskin, A., Laskin, J., Kathmann, S. M., Wise, M., Caylor, R., Imholt, F., Selimovic, V., and
587 Shilling, J. E.: Optical properties and aging of light-absorbing secondary organic aerosol, Atmospheric
588 Chemistry & Physics, 16, 1-36, 2016.
589 Liu, J., Mo, Y., Ding, P., Li, J., Shen, C., and Zhang, G.: Dual carbon isotopes ((14)C and (13)C) and optical
590 properties of WSOC and HULIS-C during winter in Guangzhou, China, Sci Total Environ, 633, 1571-1578,
591 10.1016/j.scitotenv.2018.03.293, 2018.
592 Lorenzo, R. D., Place, B. K., Vandenboer, T. C., and Young, C. J.: Composition of Size-Resolved Aged Boreal
593 Fire Aerosols: Brown Carbon, Biomass Burning Tracers, and Reduced Nitrogen, ACS Earth and Space
594 Chemistry, 2, 278-285, 10.1021/acsearthspacechem.7b00137, 2018.
595 Ma, W. L., Li, Y. F., Qi, H., Sun, D. Z., Liu, L. Y., and Wang, D. G.: Seasonal variations of sources of polycyclic
596 aromatic hydrocarbons (PAHs) to a northeastern urban city, China, Chemosphere, 79, 441-447,
597 10.1016/j.chemosphere.2010.01.048, 2010.
598 Miyazaki, Y., Kondo, Y., Takegawa, N., Komazaki, Y., Fukuda, M., Kawamura, K., Mochida, M., Okuzawa, K.,
599 and Weber, R. J.: Time-resolved measurements of water-soluble organic carbon in Tokyo, Journal of
600 Geophysical Research Atmospheres, 111, -, 10.1029/2006JD007125, 2006.
601 Moosmuller, H., Chakrabarty, R. K., and Arnott, W. P.: Aerosol light absorption and its measurement: A review, J.
602 Quant. Spectrosc. Radiat. Transf., 110, 844-878, 10.1016/j.jqsrt.2009.02.035, 2009.
603 Nakayama, T., Sato, K., Matsumi, Y., Imamura, T., Yamazaki, A., and Uchiyama, A.: Wavelength and NOx
604 dependent complex refractive index of SOAs generated from the photooxidation of toluene, Atmospheric
605 Chemistry and Physics, 13, 531-545, 10.5194/acp-13-531-2013, 2013.
606 Nguyen-Duy, D., and Chang, M. B.: Review on characteristics of PAHs in atmosphere, anthropogenic sources
607 and control technologies, Science of the Total Environment, 609, 682-693, 10.1016/j.scitotenv.2017.07.204,
608 2017.
609 Pavuluri, C. M., Kawamura, K., and Swaminathan, T.: Time-resolved distributions of bulk parameters, diacids,
610 ketoacids and α-dicarbonyls and stable carbon and nitrogen isotope ratios of TC and TN in tropical Indian
611 aerosols: Influence of land/sea breeze and secondary processes, Atmospheric Research, 153, 188-199,
612 10.1016/j.atmosres.2014.08.011, 2015.
613 Peng, J., Hu, M., Guo, S., Du, Z., Zheng, J., Shang, D., Zamora, M. L., Zeng, L., Shao, M., Wu, Y.-S., Zheng, J.,
614 Wang, Y., Glen, C. R., Collins, D. R., Molina, M. J., and Zhang, R.: Markedly enhanced absorption and
615 direct radiative forcing of black carbon under polluted urban environments, Proceedings of the National
616 Academy of Sciences of the United States of America, 113, 4266-4271, 10.1073/pnas.1602310113, 2016.
617 Ping, X., Zhou, X., Duan, J., Tan, J., He, K., Yuan, C., Ma, Y., and Zhang, Y.: Chemical characteristics of
618 water-soluble organic compounds (WSOC) in PM 2.5 in Beijing, China: 2011–2012, Atmospheric Research,
619 183, 104-112, 10.1016/j.atmosres.2016.08.020, 2017.
620 Qian, Y., Yasunari, T. J., Doherty, S. J., Flanner, M. G., Lau, W. K. M., Ming, J., Wang, H., Wang, M., Warren, S.
621 G., and Zhang, R.: Light-absorbing particles in snow and ice: Measurement and modeling of climatic and
622 hydrological impact, Advances in Atmospheric Sciences, 32, 64-91, 10.1007/s00376-014-0010-0, 2015.
623 Ren, Y., Wang, G., Wu, C., Wang, J., Li, J., Zhang, L., Han, Y., Liu, L., Cao, C., Cao, J., He, Q., and Liu, X.:
624 Changes in concentration, composition and source contribution of atmospheric organic aerosols by shifting
625 coal to natural gas in Urumqi, Atmospheric Environment, 148, 306-315, 10.1016/j.atmosenv.2016.10.053,
626 2017.

627 Saleh, R., Hennigan, C. J., McMeeking, G. R., Chuang, W. K., Robinson, E. S., Coe, H., Donahue, N. M., and
628 Robinson, A. L.: Absorptivity of brown carbon in fresh and photo-chemically aged biomass-burning
629 emissions, Atmospheric Chemistry and Physics, 13, 7683-7693, 10.5194/acp-13-7683-2013, 2013.
630 Saleh, R., Robinson, E. S., Tkacik, D. S., Ahern, A. T., Liu, S., Aiken, A. C., Sullivan, R. C., Presto, A. A., Dubey,
631 M. K., Yokelson, R. J., Donahue, N. M., and Robinson, A. L.: Brownness of organics in aerosols from
632 biomass burning linked to their black carbon content, Nature Geoscience, 7, 647-650, 10.1038/ngeo2220,
633 2014.
634 Satish, R. V., Shamjad, P. M., Thamban, N. M., Tripathi, S. N., and Rastogi, N.: Temporal Characteristics of
635 Brown Carbon over the Central Indo-Gangetic Plain, Environmental Science & Technology, 51, 6765-6772,
636 10.1021/acs.est.7b00734, 2017.
637 Shamjad, P. M., Satish, R. V., Thamban, N. M., Rastogi, N., and Tripathi, S. N.: Absorbing Refractive Index and
638 Direct Radiative Forcing of Atmospheric Brown Carbon over Gangetic Plain, ACS EARTH AND SPACE
639 CHEMISTRY, 2, 31-37, 10.1021/acsearthspacechem.7b00074, 2017.
640 Shen, G., Tao, S., Wei, S., Chen, Y., Zhang, Y., Shen, H., Huang, Y., Zhu, D., Yuan, C., Wang, H., Wang, Y., Pei,
641 L., Liao, Y., Duan, Y., Wang, B., Wang, R., Lv, Y., Li, W., Wang, X., and Zheng, X.: Field measurement of
642 emission factors of PM, EC, OC, parent, nitro-, and oxy- polycyclic aromatic hydrocarbons for residential
643 briquette, coal cake, and wood in rural Shanxi, China, Environ Sci Technol, 47, 2998-3005,
644 10.1021/es304599g, 2013.
645 Shen, Z., Zhang, Q., Cao, J., Zhang, L., Lei, Y., Huang, Y., Huang, R. J., Gao, J., Zhao, Z., Zhu, C., Yin, X.,
646 Zheng, C., Xu, H., and Liu, S.: Optical properties and possible sources of brown carbon in PM 2.5 over
647 Xi'an, China, Atmospheric Environment, 150, 322-330, 10.1016/j.atmosenv.2016.11.024, 2017.
648 Smith, J. D., Sio, V., Yu, L., Zhang, Q., and Anastasio, C.: Secondary organic aerosol production from aqueous
649 reactions of atmospheric phenols with an organic triplet excited state, Environmental Science & Technology,
650 48, 1049-1057 10.1021/es4045715, 2014.
651 Sumlin, B. J., Pandey, A., Walker, M. J., Pattison, R. S., Williams, B. J., and Chakrabarty, R. K.: Atmospheric
652 Photooxidation Diminishes Light Absorption by Primary Brown Carbon Aerosol from Biomass Burning,
653 Environmental Science & Technology Letters, 4, 540-545, 10.1021/acs.estlett.7b00393, 2017.
654 Sun, J., Zhi, G., Hitzenberger, R., Chen, Y., Tian, C., Zhang, Y., Feng, Y., Cheng, M., Zhang, Y., and Cai, J.:
655 Emission factors and light absorption properties of brown carbon from household coal combustion in China,
656 Atmospheric Chemistry and Physics, 17, 4769-4780, 10.5194/acp-17-4769-2017, 2017.
657 Teich, M., Van Pinxteren, D., Wang, M., Kecorius, S., Wang, Z., Müller, T., Močnik, G., and Herrmann, H.:
658 Contributions of nitrated aromatic compounds to the light absorption of water-soluble and particulate brown
659 carbon in different atmospheric environments, Atmospheric Chemistry and Physics, 17, 1-24,
660 10.5194/acp-17-1653-2017, 2017.
661 Wang, D., Tian, F., Yang, M., Liu, C., and Li, Y. F.: Application of positive matrix factorization to identify
662 potential sources of PAHs in soil of Dalian, China, Environmental Pollution, 157, 1559-1564,
663 10.1016/j.envpol.2009.01.003, 2009a.
664 Wang, G., Kawamura, K., Xie, M., and Hu, S.: Size-distributions of n-hydrocarbons, PAHs and hopanes and
665 their sources in the urban, mountain and marine atmospheres over East Asia, Atmospheric Chemistry &
666 Physics, 9, 8869-8882, 10.5194/acp-9-8869-2009, 2009b.
667 Wang, G., Xie, M., Hu, S., Gao, S., Tachibana, E., and Kawamura, K.: Dicarboxylic acids, metals and isotopic
668 compositions of C and N in atmospheric aerosols from inland China: implications for dust and coal burning
669 emission and secondary aerosol formation, Atmospheric Chemistry and Physics, 10, 6087-6096,

10.5194/acp-10-6087-2010, 2010.

Wang, G., Zhang, R., Gomez, M. E., Yang, L., Zamora, M. L., Hu, M., Lin, Y., Peng, J., Guo, S., Meng, J., Li, J., Cheng, C., Hu, T., Ren, Y., Wang, Y., Gao, J., Cao, J., An, Z., Zhou, W., Li, G., Wang, J., Tian, P., Marrero-Ortiz, W., Secrest, J., Du, Z., Zheng, J., Shang, D., Zeng, L., Shao, M., Wang, W., Huang, Y., Wang, Y., Zhu, Y., Li, Y., Hu, J., Pan, B., Cai, L., Cheng, Y., Ji, Y., Zhang, F., Rosenfeld, D., Liss, P. S., Duce, R. A., Kolb, C. E., and Molina, M. J.: Persistent sulfate formation from London Fog to Chinese haze, Proceedings of the National Academy of Sciences of the United States of America, 113, 13630-13635, 10.1073/pnas.1616540113, 2016.

Wang, G. H., Zhou, B. H., Cheng, C. L., Cao, J. J., Li, J. J., Meng, J. J., Tao, J., Zhang, R. J., and Fu, P. Q.: Impact of Gobi desert dust on aerosol chemistry of Xi'an, inland China during spring 2009: differences in composition and size distribution between the urban ground surface and the mountain atmosphere, Atmospheric Chemistry and Physics, 13, 819-835, 10.5194/acp-13-819-2013, 2013.

Wang, J., Cao, J., Dong, Z., Guinot, B., Gao, M., Huang, R., Han, Y., Huang, Y., Ho, S., and Shen, Z.: Seasonal variation, spatial distribution and source apportionment for polycyclic aromatic hydrocarbons (PAHs) at nineteen communities in Xi'an, China: The effects of suburban scattered emissions in winter, Environmental Pollution, 1330-1343, 10.1016/j.envpol.2017.08.106, 2017.

Wang, X., Heald, C. L., Ridley, D. A., Schwarz, J. P., Spackman, J. R., Perring, A. E., Coe, H., Liu, D., and Clarke, A. D.: Exploiting simultaneous observational constraints on mass and absorption to estimate the global direct radiative forcing of black carbon and brown carbon, Atmospheric Chemistry and Physics, 14, 17527-17583, 10.5194/acp-14-10989-2014, 2014.

Wu, C., Wang, G., Wang, J., Li, J., Ren, Y., Zhang, L., Cao, C., Li, J., Ge, S., and Xie, Y.: Chemical characteristics of haze particles in Xi'an during Chinese Spring Festival: Impact of fireworks burning, Journal of Environmental Sciences, 179-187, 10.1016/j.jes.2018.04.008, 2018.

Wu, C., Wang, G., Cao, C., Li, J., Li, J., Wu, F., Huang, R., Cao, J., Han, Y., Ge, S., Xie, Y., Xue, G., and Wang, X.: Chemical characteristics of airborne particles in Xi'an, inland China during dust storm episodes: Implications for heterogeneous formation of ammonium nitrate and enhancement of N-deposition, Environmental Pollution, 244, 877-884, 10.1016/j.envpol.2018.10.019, 2019.

Xie, M., Chen, X., Hays, M. D., Lewandowski, M., Offenberg, J., Kleindienst, T. E., and Holder, A. L.: Light Absorption of Secondary Organic Aerosol: Composition and Contribution of Nitroaromatic Compounds, Environmental Science & Technology, 51, 11607-11616, 10.1021/acs.est.7b03263, 2017.

Xie, M., Shen, G., Holder, A. L., Hays, M. D., and Jetter, J. J.: Light absorption of organic carbon emitted from burning wood, charcoal, and kerosene in household cookstoves, Environmental Pollution, 240, 60-67, 10.1016/j.envpol.2018.04.085, 2018.

Yan, C., Zheng, M., Sullivan, A. P., Bosch, C., Desyaterik, Y., Andersson, A., Li, X., Guo, X., Zhou, T., and Örjan, G.: Chemical characteristics and light-absorbing property of water-soluble organic carbon in Beijing: Biomass burning contributions, Atmospheric Environment, 121, 4-12, 10.1016/j.atmosenv.2015.05.005, 2015.

Yan, C., Zheng, M., Bosch, C., Andersson, A., Desyaterik, Y., Sullivan, A. P., Collett, J. L., Zhao, B., Wang, S., He, K., and Gustafsson, O.: Important fossil source contribution to brown carbon in Beijing during winter, Scientific Reports, 7, 43182, 10.1038/srep43182, 2017.

Yan, J., Wang, X., Gong, P., Wang, C., and Cong, Z.: Review of brown carbon aerosols: Recent progress and perspectives, Science of The Total Environment, 634, 1475-1485, 10.1016/j.scitotenv.2018.04.083, 2018.

Yang, H., Xu, J., Wu, W. S., Wan, C. H., and Yu, J. Z.: Chemical Characterization of Water-Soluble Organic

Aerosols at Jeju Island Collected During ACE-Asia, Environmental Chemistry, 1, 13-17, 10.1071/EN04006, 2004.

Yuan, B., Liggio, J., Wentzell, J., Li, S.-M., Stark, H., Roberts, J. M., Gilman, J., Lerner, B., Warneke, C., Li, R., Leithead, A., Osthoff, H. D., Wild, R., Brown, S. S., and de Gouw, J. A.: Secondary formation of nitrated phenols: insights from observations during the Uintah BasinWinter Ozone Study (UBWOS) 2014, Atmospheric Chemistry and Physics, 16, 2139-2153, 10.5194/acp-16-2139-2016, 2016.

Zhai, J., Lu, X., Li, L., Zhang, Q., Zhang, C., Chen, H., Yang, X., and Chen, J.: Size-resolved chemical composition, effective density, and optical properties of biomass burning particles, Atmospheric Chemistry and Physics, 17, 1-25, 10.5194/acp-17-7481-2017, 2017.

Zhang, X., Hecobian, A., Zheng, M., Frank, N. H., and Weber, R. J.: Biomass burning impact on $PM_{2.5}$ over the southeastern US during 2007: integrating chemically speciated FRM filter measurements, MODIS fire counts and PMF analysis, Atmospheric Chemistry and Physics, 10, 6839-6853, 10.5194/acp-10-6839-2010, 2010.

Zhang, X., Lin, Y. H., Surratt, J. D., Zotter, P., Prévôt, A. S. H., and Weber, R. J.: Light-absorbing soluble organic aerosol in Los Angeles and Atlanta: A contrast in secondary organic aerosol, Geophysical Research Letters, 38, 759-775, 10.1029/2011GL049385, 2011.

Zhang, Y., and Tao, S.: Global atmospheric emission inventory of polycyclic aromatic hydrocarbons (PAHs) for 2004, Atmospheric Environment, 43, 812-819, 10.1016/j.atmosenv.2008.10.050, 2009.

Zhang, Z., Gao, J., Engling, G., Tao, J., Chai, F., Zhang, L., Zhang, R., Sang, X., Chan, C. Y., and Lin, Z.: Characteristics and applications of size-segregated biomass burning tracers in China's Pearl River Delta region, Atmospheric Environment, 102, 290-301, 10.1016/j.atmosenv.2014.12.009, 2015.

Zhao, M., Huang, Z., Qiao, T., Zhang, Y., Xiu, G., and Yu, J.: Chemical characterization, the transport pathways and potential sources of PM2.5 in Shanghai: Seasonal variations, Atmospheric Research, 158-159, 66-78, 10.1016/j.atmosres.2015.02.003, 2015a.

Zhao, R., Lee, A. K. Y., Huang, L., Li, X., Yang, F., and Abbatt, J. P. D.: Photochemical processing of aqueous atmospheric brown carbon, Atmospheric Chemistry and Physics, 15, 6087-6100, 10.5194/acp-15-6087-2015, 2015b.

Zong, Z., Wang, X., Tian, C., Chen, Y., Qu, L., Ji, L., Zhi, G., Li, J., and Zhang, G.: Source apportionment of PM2.5 at a regional background site in North China using PMF linked with radiocarbon analysis: insight into the contribution of biomass burning, Atmospheric Chemistry and Physics, 16, 11249-11265, 10.5194/acp-16-11249-2016, 2016.

Table List

Figure caption

PMF analysis due to the limited number of samples).

Fig. 8 Source apportionment for airborne fine particulate BrC in Xi'an during the campaign.

Table 1. Concentrations of organic carbon in $PM_{2.5}$ and meteorological conditions during winter and summer of 2017 in Xi'an, inland China.

	Winter	Summer
I. Mass concentrations of organic matter in $PM_{2.5}$		
WSOC ($\mu gC/m^3$)	23 ± 13	5.8 ± 1.4
OC ($\mu gC/m^3$)	41 ± 25	8.4 ± 2.4
PAHs (ng/m^3)	149± 89	8.1 ± 6.5
OPAHs (ng/m^3)	174 ± 98	17 ± 8.7
Nitrophenols (ng/m^3)	17± 12	0.40 ± 0.27
Levoglucosan (ng/m^3)	739 ± 432	29 ± 22
II. $PM_{2.5}$ and meteorological parameters		
$PM_{2.5}$ ($\mu g/m^3$)	194 ± 141	37 ± 16
T (°C)	2.6 ± 2.9	31 ± 5.4
RH (%)	60± 20	58 ± 19
Visibility (km)	7.0 ± 7.0	21 ± 11

822 Table 2. Comparison on light absorption ($abs_{\lambda=365nm}$), MAC, and AAE values of water-extracts of
823 $PM_{2.5}$ in Xi'an, China with those in other cities.

Location	Time	$abs_{\lambda=365nm}$ (M/m)		MAC (m^2/g)		AAE		References
		Winter	Summer	Winter	Summer	Winter	Summer	
Xi'an, China	2016-2017	49±32[a]	5.2±2.1[a]	1.3±0.03[a]	0.8[a]±0.1[a]	6.1±9.7[a]	5.5±8.8[a]	This study
		28±16	3.5±1.7	1.2±0.06	1.1±0.2	5.3±8.5	4.8±7.7	
	2008-2009	46±20[a]	8.3±2.3[a]	1.3[a]	0.7[a]	6.0[a]	6.0[a]	Huang et al. (2018)
		25±12	5.0±1.3	1.7	1.0	5.7	5.7	
	2010-2011	10±8.6	3.7±3.8	1.3	0.5			Du et al. (2014)
Beijing, China	2011	10±6.9		1.2		7.3		Cheng et al. (2016)
	2013	14±5.2	4.6±2.2	1.5	0.7	5.3	5.8	Yan et al. (2015)
Nanjing, China	2015-2016	9.4 ± 4.7	3.3±2.4	1.0	0.5	6.7	7.3	Chen et al. (2018)
Guangzhou, China	2012	3.6±1.3		0.8		5.3		Liu et al. (2018)
Delhi, India	2010-2011			1.6		5.1		Kirillova et al. (2014)
	2015-2016	24±19		1.2				Satish et al. (2017)
Indo- Gangetic Plain India	2011	40 ± 18[b]		1.3[b]		5.1[b]		Bachi et al. (2016)
		52 ± 27[c]		1.3[c]		5.3[c]		
Seoul, Korea	2013-2013	11[a]	5.8[a]	0.9[a]	1.5[a]	5.5[a]	4.1[a]	Kim et al.(2016)
		7.3	0.9	1.0	0.3	5.8	8.7	
Atlanta, US	2010		0.6±0.4		1.2-0.2		3.4	Zhang et al. (2011)
Los Angeles Basin, US	2010		0.4-1.6		0.7		7.6	Zhang et al. (2013)

824 Notes: [a] solution extracted by MeOH; [b] samples collected at day time; [c] samples collected in the night
825
826
827
828
829
830
831 Table 3. Complex refractive index (k) of brown carbon from samples extracted by water in
832 two seasons.

Particle size (μm)	Winter	Summer
1.31	0.047 ± 0.005	0.021 ± 0.010
0.73	0.048 ± 0.008	0.033 ± 0.010
0.45	0.048 ± 0.013	0.031 ± 0.009
0.18	0.038 ± 0.016	0.026 ± 0.008

833
834
835

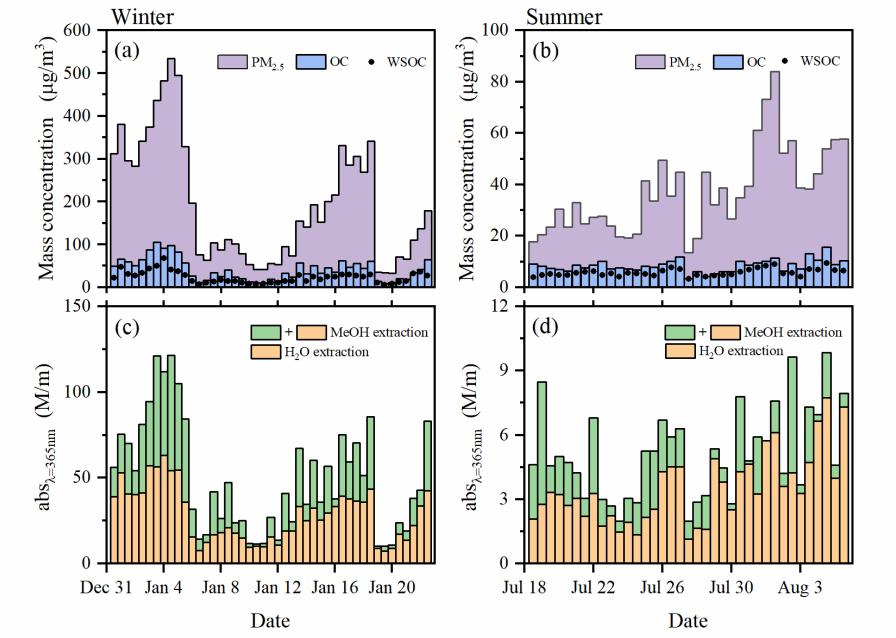

Fig. 1 Temporal variations of WSOC, OC, $PM_{2.5}$, and $abs_{\lambda=365nm}$ of $PM_{2.5}$ samples extracted by water (H_2O-extraction) and methanol (MeOH-extraction) during winter (**a** and **c**) and summer (**b** and **d**).

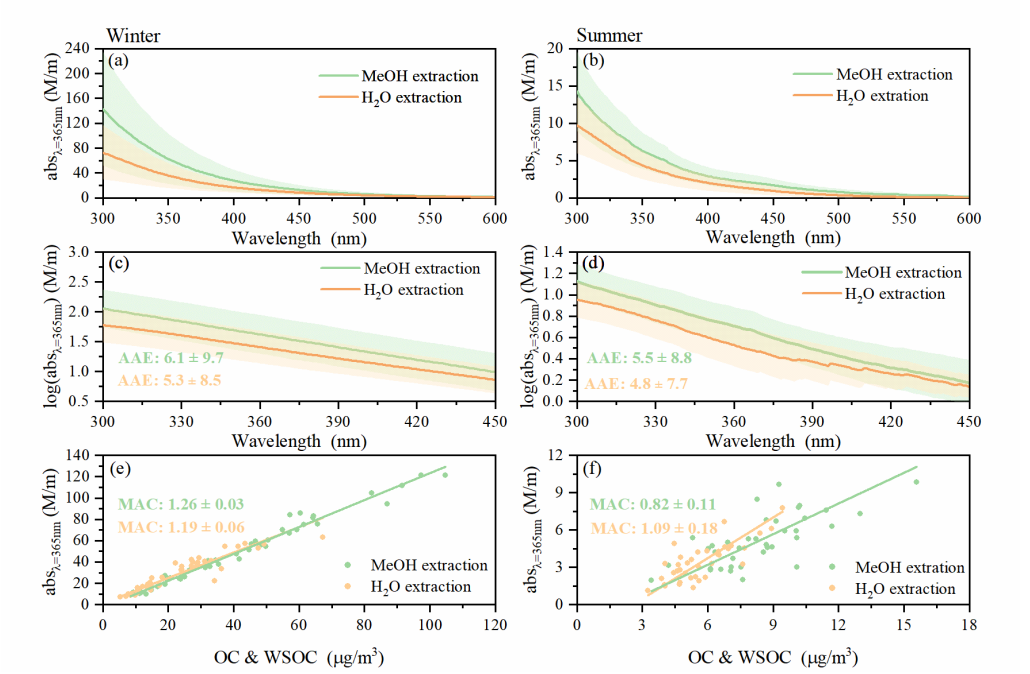

Fig. 2 Seasonal average values of $abs_{\lambda=365nm}$, AAE, and MAC extracted by MeOH and H_2O. AAE is calculated by linear regression fit log ($abs_{\lambda=365nm}$) versus log(λ) in the wavelength range of 300–450 nm. (The shadows indicating the standard deviations)

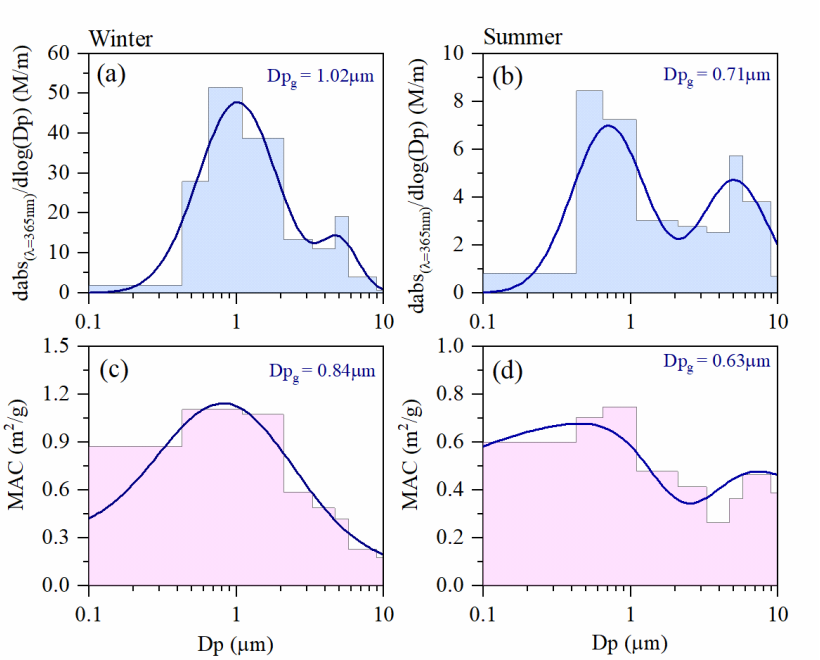

Fig. 3 Size distributions of $abs_{\lambda=365nm}$ and MAC of $PM_{2.5}$ samples extracted by water during the winter and summer of 2017 in Xi'an.

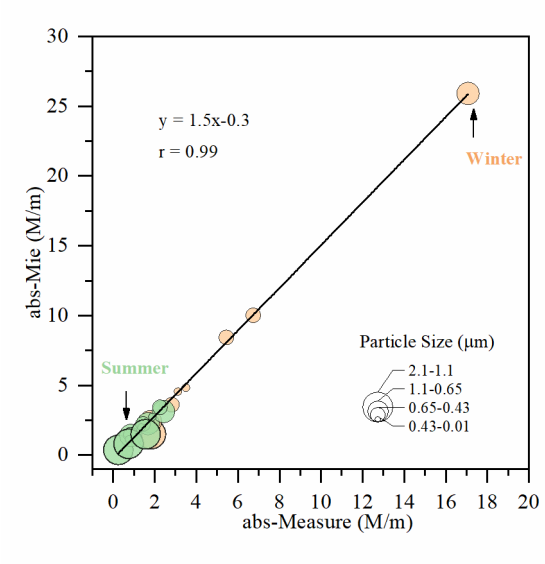

Fig. 4 An orthogonal regression analysis for $abs_{\lambda=365nm}$ of samples between predicted by Mie theory and extracted by water for different particle size (Dp < 2.1μm).

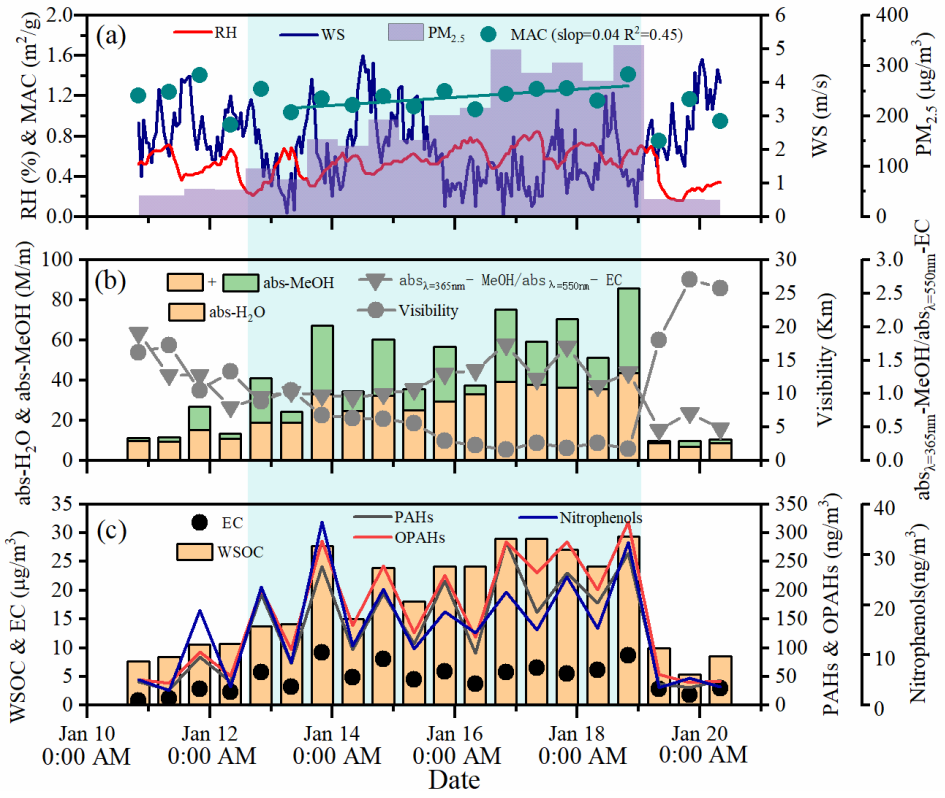

Fig. 5 Temporal variations of $PM_{2.5}$, meteorological parameters, $abs_{\lambda=365nm}$ of W(M)SOC and organic compounds in the period of January 10th -20th (The cyan shadow indicates a haze period from January 12th to 19th with a daily $PM_{2.5}$ > 75 μg/m^3).

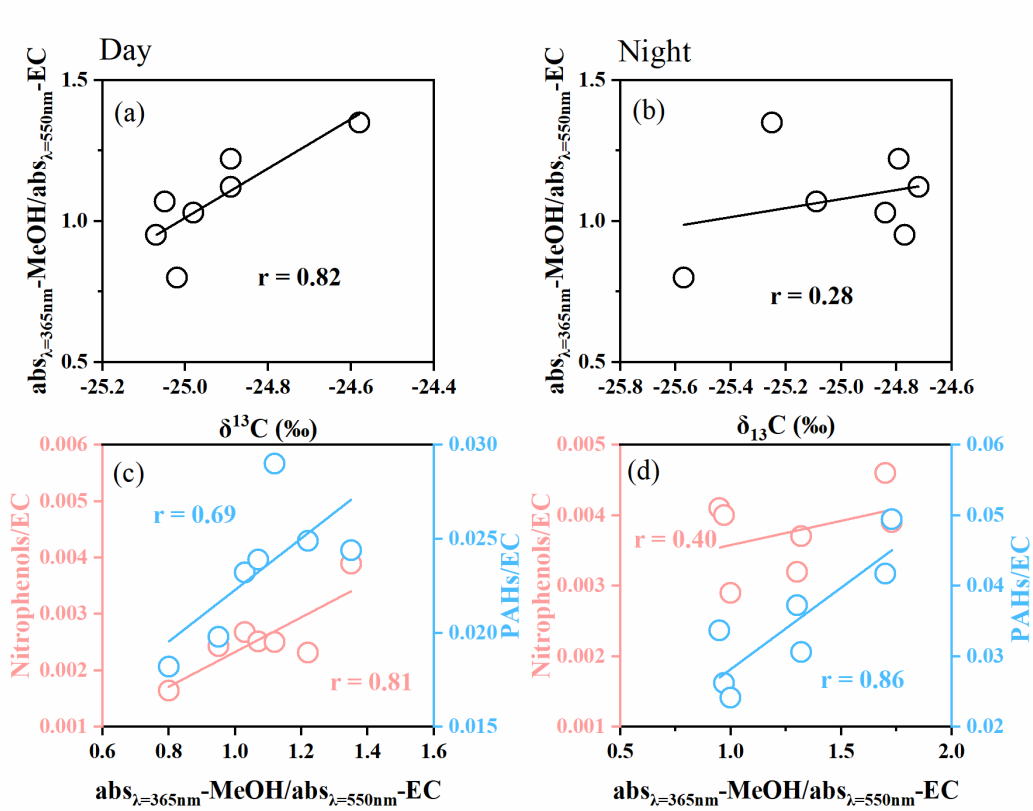

Fig.6 Linear fit regressions for the ratio of light absorption of methnoal-extracts to light absorption of EC ($abs_{\lambda=365nm}$-MeOH/$abs_{\lambda=550nm}$-EC) with (**a** and **b**) $\delta^{13}C$ and (**c** and **d**) relative abundance of nitrophenol to EC(Nitrophenol/EC) in the day- and night-$PM_{2.5}$ samples collected during the haze period of January 12th to19th (corresponding to the cyan shadow in Figure 5) in Xi'an.

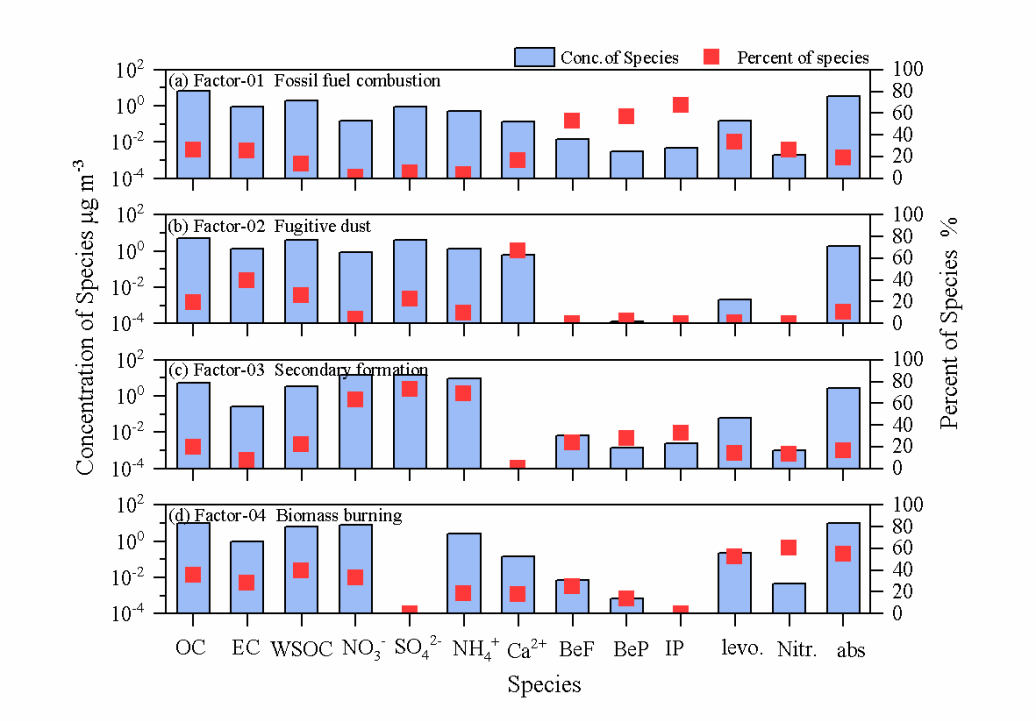

Fig. 7 Factor profiles resolved by PMF mode during the winter and summer sampling period. The bars represent the concentrations of species and the dots represent the contributions of species appointed to the factors (the summer and winter samples were merged together for the PMF analysis due to the limited number of samples).

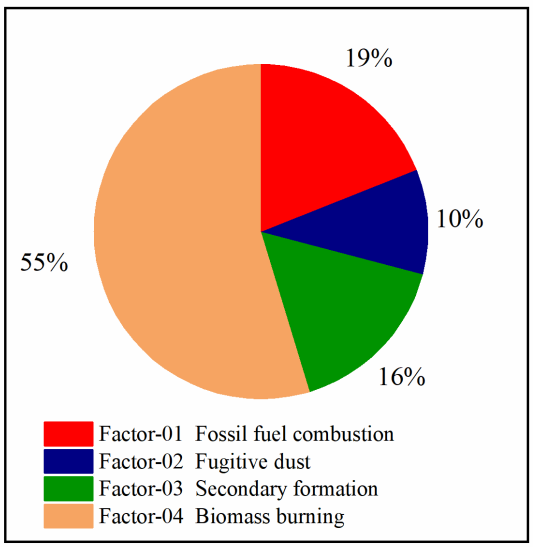

Fig. 8 Source apportionment for airborne fine particulate BrC in Xi'an during the campaign.